Vol 16 No 11, November 2007
1009-1963/2007/16(11)/3328-04

Chinese Physics

© 2007 Chin. Phys. Soc.
and IOP Publishing Ltd

Phase transformation and nanograting structure on TiO_2 rutile single crystal induced by infrared femtosecond laser*

Ma Hong-Liang(马洪良)[a)], Yang Jun-Yi(杨俊毅)[a)], Lu Bo(鲁 波)[a)], and Ma Guo-Hong(马国宏)[b)]

[a)] *Instrumental Analysis & Research Center, Shanghai University, Shanghai* 200444, *China*

[b)] *Department of Physics, Shanghai University, Shanghai* 200444 *China*

(Received 4 January 2007; revised manuscript received 27 January 2007)

In this paper, Titanium dioxide (TiO_2) rutile single crystal was irradiated by infrared femtosecond laser pulses with repetition rate of 250 kHz. For a P-polarized femtosecond laser, the periodic nanograting structure on the ablation crater surface was formed . The periodicity is much less than the laser wavelength. The direction of nanograting alignment depends on the polarization laser beam. Micro-Raman spectra show that the intensity of E_g Raman vibrating mode of rutile phase increases and that of A_{1g} Raman vibrating mode decreases apparently within the ablation crater. With the increase of irradiation time and laser average power, the Raman vibrating modes of anatase phase emerged. Rutile phase of TiO_2 single crystal is partly transformed into anatase phase.

Keywords: infrared femtosecond laser, titanium dioxide single crystal, phase transformation, micro-Raman spectroscopy

PACC: 3300, 3390

1. Introduction

Titanium dioxide (TiO_2) is a large-band gap semiconductor with important applications in corrosion-resistant coating, pigment, photocatalysis, gas sensors, medical implants and optical active coatings and solar energy conversion.[1−4] It is well-known that TiO_2 exists three natural phases: rutile, anatase, and brookite.[5] Every titanium is surrounded by six oxygens to form a TiO_6 octahedron in the modifications, but they have different networks composed of TiO_6 octahedra. A lot of studies have been carried out on the formation of rutile and anatase crystals.[6−9] At elevated pressures TiO_2 has a rich phase diagram with a series of structural phase transformations. The structure and stability of the high-pressure phases of TiO_2 are of particular interest in Earth sciences, for these phases are an accessible analogue of minerals in the Earth's mantle. Rutile TiO_2 is particularly attractive in this context because it is expected to undergo a sequence of phase transformations with increasing pressure similar to that experienced by SiO_2 in the Earth's lower mantle. High pressure x-ray-diffraction[10−12] and Raman spectroscopy[13,14] studies have revealed that rutile and anatase transform to a columbite structure at high pressure. Recently phase of TiO_2 from anatase to rutile is studied by UV Raman spectroscopy excited by 325 nm and 244 nm lasers.[15] But there are no attempts to phase transformation of TiO_2 from rutile to anatase by using infrared femtosecond laser pulses.

During the last decades, special interest was paid to the potential of ultrashort laser pulses with durations in the picosecond to femtosecond domain with respect to laser-induced phase transitions[16−18] as well as to the fundamental processes during laser ablation. The femtosecond laser, because of ultrashort pulse and ultrahigh peak power, has exhibited great potentials in material processing and many microstructures in transparent materials have been fabricated, including optical waveguides, splitters, couples, three-dimensional data storage, and photon crystals.[19−23] Femtosecond laser can be used to generate a number of nonlinear effects by multiphoton absorption and avalanche ionization in the focusing area of materials.

*Project supported by Shanghai Leading Academic Discipline Project, China (Grant No T0104), the Shanghai Nano-technology Promotion Center and Science & Technology of Shanghai Municipality, China (Grant No 0652nm005), Science Foundation of Shanghai Municipal Commission Education and Science and Technology Commission of Shanghai Municipal, China (Grant No 06PJ14042).

2. Experiment

We used a commercial 250 kHz femtosecond (fs) laser system based on a regenerative Ti:sapphire amplifier using chirped pulse amplification technique (RegA 9000, Coherent) delivering 6 μJ, 120 fs laser pulses at a centre wavelength of 800 nm (photon energy 1.55 eV). The Gaussian laser pulses were focused by an optical micro-objective lens (Olympus BX51) with a numerical aperture NA of 0.46, yielding a focus diameter $d_{\text{focus}} = 1.22\lambda/\text{NA} = 1.22 \times 800\ \text{nm}/0.46 \approx 2.12\ \mu\text{m}$. Using a CCD camera system we find that the focus of the fs-laser beam can be positioned directly on the sample located on a positioning stage. So the sample can be moved in x, y, z-directions. The average output power can be changed continuously with a Glan polarizer. A mechanical shutter was used to select laser pulses from a pulse-train, as shown in Fig.1.

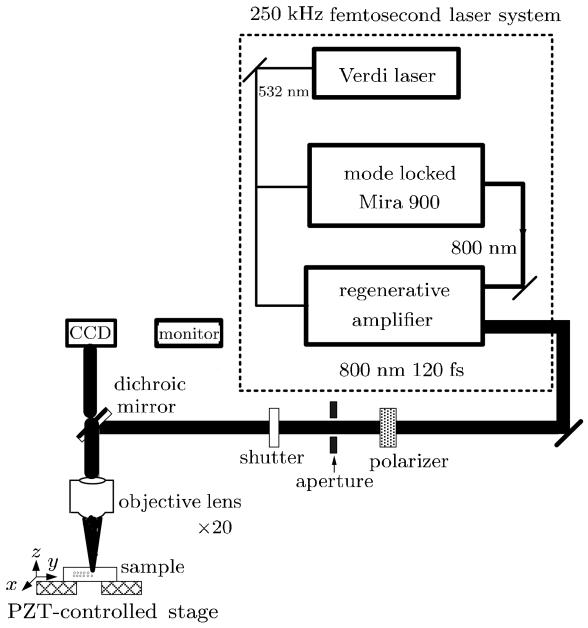


Fig.1. Experimental set-up of the fs-IR-laser irradiation facility with PZT-controlled stage.

Rutile TiO_2 single crystal sample prepared in optical floating zone systems (Z-T-10000-H-VI-P-SH, Japan) is 10 mm in diameter and 1.5 mm thick. It is polished on both sides. The specimen was mounted on a motorized xyz-translation stage and had a position which is perpendicular to the direction of laser incidence. The morphology of the ablation crater is measured with scanning electronic microscope (SEM).

The phase transformation of TiO_2 rutile single crystal induced by the fs-IR-laser irradiation was analysed by micro-Raman spectroscopy (in Via-plus, Renishaw). The Raman spectra were excited by the 514nm radiation of an argon ion laser operating at 20 mW. A 50× objective lens was used to focus the beam onto the sample. Spectra were recorded at room temperature. The scattered light was then collected, dispersed and detected by a standard CCD array detector. The Rayleigh scattered light was reduced by a notch filter. The spectra were recorded by using a 1800 groove mm^{-1} grating giving a spectral resolution better than 1 cm^{-1}. The spectrum scattering detection region ranges from 100 cm^{-1} to 900 cm^{-1}.

3. Experimental results and discussion

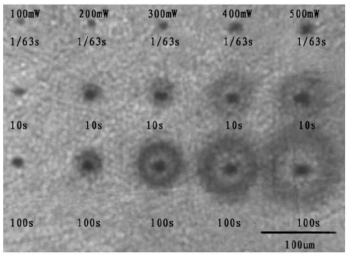


Fig.2. Microscope photograph of the ablation craters induced by 800nm fs pulse laser on the surface of rutile single crystal.

Figure 2 shows the visible laser-damage spots on the surface of rutile single crystal induced by femtosecond laser pulses. Laser average power on the surface of the sample is from 100 mW to 500 mW and the irradiation time is from 1s/63 to 100s. Due to the interaction of a laser with matter at intensity above the ionization threshold, the plasma generated in the focal region increases the absorption coefficient and produces a fast energy release in a very small volume. A strong shock wave is generated in the interaction region and this propagates into the surrounding cold material. The shock wave propagation is accompanied by compression of the solid material at the wave front and decompression behind it, which leads to the formation of an ablation crater on the surface. Because of the accumulation effect, with the increase of pulse number, the temperature in the focal volume would rise accordingly, and then the thermal energy diffuses from the focal point to the outer area and the heated region begins melting and expanding. Due to the high temperature and pressure formed in the focal volume, the material at the edge of the modified region is compressed between the expanding region and the unheated one, and the refractive index of the compressed region increases, while the density of the

expanding region reduces. The energy deposits in the central region, the circular structure with high refractive index emerges between the expanding region and the unheated one.

Figure 3(a) shows the SEM image of the ablation crater irradiated by P-polarized laser pulses at the average power of 200mW. The nanogratings with period of about 120nm aligned in a direction perpendicular to the electric field of light wave have been observed on the ablation crater. When the direction of light polarization was moved likewise 45°, the direction of the nanogratings alignment moved 45° along light polarization, shown in Fig.3.(b), and grating period of 180nm was observed. The grating periods at different laser energy and different laser pulses are under investigation.

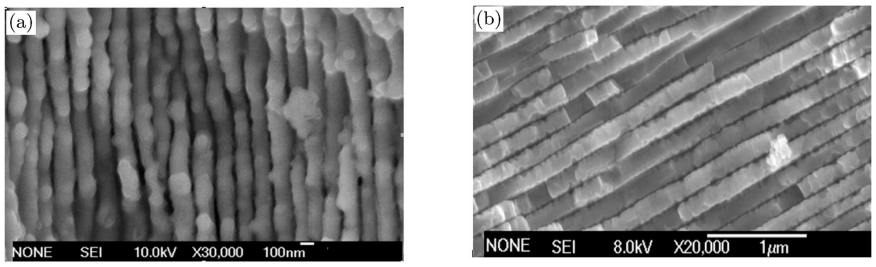


Fig.3. SEM images of the periodic nanostructures with laser polarization at 0° with laser average power of 200 mW (a), and 45°, with laser power of 100 mW (b).

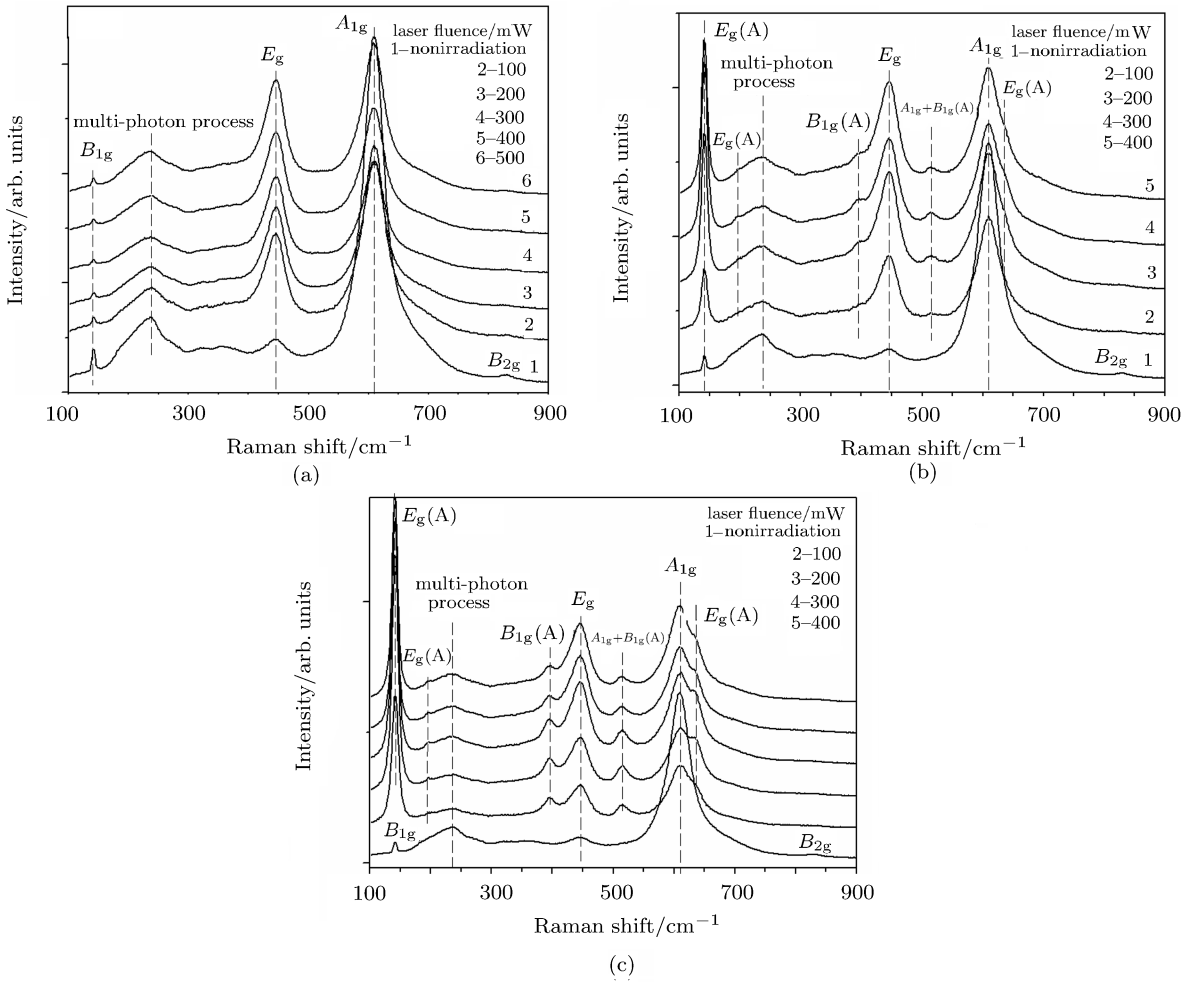


Fig.4. Raman spectra of TiO_2 single crystal irradiated by fs-laser pulses at different average powers from 100mW to 500 mW. Irradiation time is 1s/63 (a), 10s (b), and 100s(c).

Such gratings are generated as a result of interference between the light field and the surface plasmon-polariton wave. A variety of nonlinear processes occurs in the interaction of femtosecond laser pulses with solids.[24,25] The periods of our nanostructure are nearly equal to the wavelength of second harmonics in sample. We believe that it is induced by the interference of the surface scattered laser beams and the second harmonic laser with the wavelength of 400 nm generated at the sample surface. The period Λ is

$$\Lambda = \lambda/2n, \tag{1}$$

where n is the refractive index. Second harmonic generation was also proposed to play some role in the formation of nanostructures in compound semiconductors.[26]

The rutile structure belongs to the P42/mnm tetragonal space group. There are five Raman active modes: B_{1g}, multi-photon process, E_g, A_{1g} and B_{2g}. Figure 4 shows the Raman spectra before irradiation and after irradiation by using femtosecond laser pulses. In Fig.4(a), the bottom line is the Raman shifts of rutile crystal before irradiation, exhibiting dominant peaks at 140.2, 235.5, 445.8, 609.5, and 825.5 cm^{-1}, which are assigned to the five Raman active modes of rutile single crystal.[27] When irradiation time is $\frac{1}{63}$ s, the ratio between the intensity of E_g mode and A_{1g} mode increases with the increase of laser average power and the intensity of Raman E_g mode increases and up to nearly equal to that of A_{1g} mode. High fluence neutron irradiation and proton irradiation induce similar variations of the frequency and intensity of Raman vibration modes in the rutile single crystals.[28] When irradiation time is 10s, the anatase phase occurs and the intensity of Raman E_g(A) mode increases apparently with the increase of laser average power from 100 mW to 500 mW, as shown in Fig.4(b). Figure 4(c) shows a E_g(A) mode (632.7 cm^{-1}) at irradiation time of 100s.

In conclusion, we find that tightly focused 120 fs laser pulses initiate TiO_2 rutile phase transformation into anatase produced by the high pressure due to micro-explosions on the TiO_2 crystal surface. The extreme conditions produced in the micro-explosions can serve as a novel phase transformation study for high pressure and high temperature, and the material processing. Nanogratings formed on the crystal surface irradiated by P-polarized fs pulse laser were observed. The grating periods at different laser energy and different laser pulses are under investigation.

References

[1] Fujishima A and Honda K 1972 *Nature* **238** 37
[2] Fox M A and Dulay M T 1993 *Chem. Rev.* **93** 341
[3] GräNtzel M 2001 *Nature* **414** 338
[4] Li B, Zhao J, Onda K, Jorden K D, Yang J and Petek L H 2006 *Science* **311** 1436
[5] Mo S D and Ching W Y 1995 *Phys. Rev.* B **51** 13023
[6] Chang H and Huang P J 1998 *J. Raman Spectr.* **29** 97
[7] Cronemeyer D C 1952 *Phys. Rev.* **87** 876
[8] S Porto P S, Fleury P A and Damen T C 1967 *Phys. Rev.* **154** 522
[9] Swamy V, Kuznetsov A, Dubrovinsky L S, Caruso R A, Shchukin D G and Muddle B C 2005 *Phys. Rev.* B **71** 184302
[10] McQueen R G, Jamieson J C and Marsh S P 1967 *Science* **155** 1401
[11] Olsen J S, Jiang J Z and Gerward L 1999 *J. Phys. Chem. Solids* **60** 229
[12] Arlt T, Bermejo M, Blanco M A, Gerward L, Jiang J Z, Olsen J S and Recio J M 2000 *Phys. Rev.* B **61** 14414
[13] Mammone J F, Sharma S K and Nicol M 1980 *Solid State Commun.* **34** 799
[14] Lagarec K and Desgreniers S 1995 *Solid State Commun.* **94** 519
[15] Zhang J, Li M, Feng Z, Chen J and Li C 2006 *J. Phys. Chem.* B **110** 927
[16] Shank C V, Yen R and Hirlimann C 1983 *Phys. Rev. Lett.* **50** 454
[17] Ge Y C 2006 *Chin. Phys.* **15** 2909
[18] Yan L X, Zhang Y S, Zheng G X, Liu J R, Cheng J P and Lu M 2006 *Chin. Phys.* **15** 2271
[19] Davis K M, Miura K, Sugimoto N and Hirao K 1996 *Opt. Lett.* **21** 1729
[20] Miura K , Qiu J R, Inouva H, Mitsugu T and Hirao K 1997 *Appl. Phys. Lett.* **71** 3329
[21] Glezer E N and Mazur E 1997 *Appl. Phys. Lett.* **71** 882
[22] Tang Y Z, Jia K M, Li B Y, Yang J Y, Jiang X Q, Wu Y M and Wang Y L 2004 *Chin. Phys. Lett.* **21** 1061
[23] McPhail D, Straub M and Gu M 2005 *Appl. Phys. Lett.* **87** 091117
[24] Jia T Q, Zhao F L, Huang M, Chen H X, Qiu J R, Li R X, Chen Z Z and Kuroda H 2006 *Appl. Phys. Lett.* **88** 111117
[25] Tinten K S and Linde D 2000 *Phys. Rev.* B **61** 2643
[26] Borowiec A and Haugen H 2003 *Appl. Phys. Lett.* **82** 4462
[27] Arsov Lj D, Kormann C and Plieth W 1991 *J. Raman Spectr* **22** 573
[28] Lu T C, Lin L B, Zu X T, Zhu S and Wang L M 2004 *Nucl. Instr. & Meth. Phys. Res.* B **218** 111